Medicinal Chemistry

DOI: 10.1002/anie.200702961

Potent Inhibitors of tRNA-Guanine Transglycosylase, an Enzyme Linked to the Pathogenicity of the *Shigella* Bacterium: Charge-Assisted Hydrogen Bonding**

Simone R. Hörtner, Tina Ritschel, Bernhard Stengl, Christian Kramer, W. Bernd Schweizer, Björn Wagner, Manfred Kansy, Gerhard Klebe, and François Diederich**

Dedicated to Professor Dieter Seebach on the occasion of his 70th birthday

tRNA-Guanine transglycosylase (TGT, EC 2.4.2.29) is a tRNA-modifying enzyme common to nearly all organisms including humans.[1] In bacteria, TGT catalyzes the exchange of guanine in position 34 by preQ$_1$, whereas eukaryotic TGT accelerates the replacement by queuine.[2] This difference in substrate specificity offers the possibility for selective inhibition of the bacterial enzyme, which has been linked to the pathogenicity of *Shigella*, the causative agent of bacillary dysentery (Shigellosis), a diarrheal disease responsible for more than a million deaths annually.[3] As substantial crystallographic and biochemical information about the bacterial enzyme is available, TGT represents an ideal target for structure-based drug design to facilitate the development of selective antibiotics against bacillary dysentery.

We recently introduced *lin*-benzoguanine (**1**)[4,5] as a nucleobase analogue to fill the pocket occupied by preQ$_1$ (Figure 1, and the Supporting Information).[6] This heterotricyclic skeleton fully maintains the hydrogen-bonding pattern of the natural substrate (Figure 1a) and shows mixed competitive–uncompetitive inhibition with respect to tRNA binding (competitive inhibition constant $K_{ic} = 4.1\ \mu M$, uncompetitive inhibition constant $K_{iu} = 7.9\ \mu M$; against *Zymomonas (Z.) mobilis* TGT).[4] We focused our first design attempts on the filling of a neighboring shallow hydrophobic pocket occupied by the ribose 34 moiety of the natural substrate. This pocket is lined by Val282, Leu68, and Val45. Lipophilic residues such as phenethyl were therefore introduced at position 4 of *lin*-benzoguanine (Figure 1b, see Scheme 1 for numbering). While the predicted orientation of the lipophilic vectors into this pocket was confirmed by X-ray

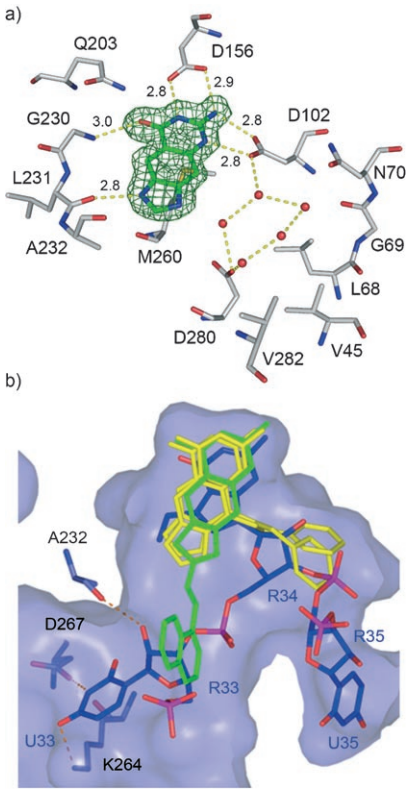

Figure 1. a) Binding mode of *lin*-benzoguanine (**1**) in the active site of TGT.[4,5] The two catalytic aspartates Asp280 and Asp102 are solvated by an unperturbed water cluster (protein data base (PDB) code: 2BBF, resolution 1.7 Å). Dashed lines indicate hydrogen bonds; distances between heavy atoms in Å. Ligand skeleton green; C gray; O red; N blue; S yellow. b) Superimposition of TGT in complex with modified tRNA (blue backbone, PDB-code 1Q2S, resolution 3.2 Å),[6] 4-phenethyl-substituted *lin*-benzoguanine (yellow, PDB-code: 1Y5V, resolution 1.58 Å), and inhibitor **8** (green, PDB-code: 2QZR, resolution 1.95 Å). For the TGT-tRNA complex, the U33-preQ$_1$-U35 fragment bound to the active site is shown. The 4-phenethyl substituent orients towards the ribose 34 binding pocket; two preferred conformations are shown. In contrast, the naphthylmethylamino substituent of **8** points into the ribose 33 binding pocket. Figures were prepared using PyMOL.[17]

[*] S. R. Hörtner, C. Kramer, Dr. W. B. Schweizer, Prof. Dr. F. Diederich
Laboratory of Organic Chemistry, ETH Zürich
Hönggerberg, HCI, 8093 Zürich (Switzerland)
Fax: (+41) 44-632-1109
E-mail: diederich@org.chem.ethz.ch

T. Ritschel, Dr. B. Stengl, Prof. Dr. G. Klebe
Institute of Pharmaceutical Chemistry
Philipps-University Marburg
Marbacher Weg 6, 35032 Marburg (Germany)
Fax: (+49) 6421-282-8994
E-mail: klebe@mailer.uni-marburg.de

B. Wagner, Dr. M. Kansy
Pharmaceuticals Division, Discovery Chemistry
F. Hoffmann-La Roche AG, 4070 Basel (Switzerland)

[**] Work at Zürich was supported by the ETH Research Council and the Fonds der Chemischen Industrie, work at Marburg by the Deutsche Forschungsgemeinschaft.

Supporting information for this article is available on the WWW under http://www.angewandte.org or from the author.

crystallography, binding efficacy of the inhibitors, whose mechanism of action was fully competitive, remained in the micromolar range (e.g. $K_i = 1\ \mu M$ for the phenethyl-substituted ligand). An extended crystallographic investigation[5] subsequently revealed that the lipophilic vector introduced into position 4 of the heterocyclic scaffold disrupted a highly conserved water network solvating the two catalytic aspartates Asp 280 and Asp 102 (Figure 1 a). Apparently, energetic gains from the ligand's complementary occupation of the prominent shallow hydrophobic pocket were fully compensated by energetic costs arising from the clearly unfavorable disruption of the water network and violation of the solvation requirements of the two catalytic Asp side chains.

To avoid this serious problem and to enhance binding efficacy, we subsequently concentrated our design towards the introduction of liphophilic vectors at position 2 of the *lin*-benzoguanine skeleton. Molecular modeling using MOLOC[7] suggested these substituents to point towards the pocket accommodated by the ribose 33 residue of the substrate (rather than ribose 34). It was therefore expected to leave the solvation water network of the two Asp side chains intact. Based on the modeling considerations regarding space and environmental polarity of the ribose 33 site, ligands **2**–**12** with various alkylamino- and arylalkylamino substituents were designed (Table 1). Compounds **2**–**4** with small residues were prepared as initial controls to estimate experimentally the gain in binding free enthalpy resulting from penetration and increasing occupation of the ribose 33 pocket by larger residues. The introduction of morpholine moieties in **11** and **12** was intended to give full water solubility of the notoriously poorly soluble *lin*-benzoguanine derivatives, which is required for planned cell-based assays.

Table 1: 2-Substituted *lin*-benzoguanine derivatives prepared for the inhibition of TGT.

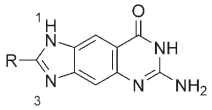

Compd.	R	K_i [nM]	Compd.	R	K_i [nM]
1	H	4100 ± 1000	**7**[a]	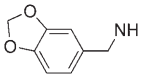	35 ± 6
2	Me	1600 ± 400	**8**[a]	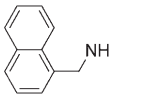	55 ± 11
3	NH_2	77 ± 12	**9**	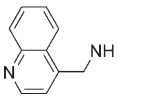	27 ± 12
4		58 ± 36	**10**[a]	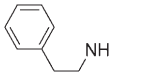	10 ± 3
5[a]	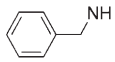	70 ± 1	**11**[b]	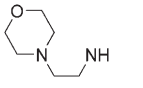	6 ± 6
6[a]	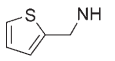	35 ± 9	**12**[b]	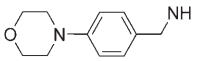	40 ± 18

[a] Isolated and used as the bis(trifluoroacetate) salt (TFA = CF_3COOH). [b] Isolated and used as the tris(trifluoroacetate) salt.

The synthesis of the representative 2-benzylamino-substituted *lin*-benzoguanine **5** is shown in Scheme 1 (for the synthesis and characterization of the other new ligands, see the Supporting Information). Esterification of commercially

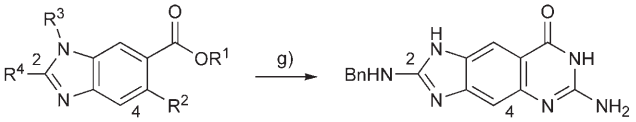

		R^1	R^2	R^3	R^4
a)	**13**	H	H	H	H
b)	**14**	Me	H	H	H
c)	**15**	Me	NO_2	H	H
d)	**16a**	Me	NO_2	SO_2NMe_2	H
e)	**17a**	Me	NO_2	SO_2NMe_2	Br
f)	**18**	Me	NO_2	SO_2NMe_2	NHBn
	19	Me	NH_2	SO_2NMe_2	NHBn

Scheme 1. Synthesis of ligand **5**. a) $SOCl_2$, MeOH, 65 °C, 92 %; b) HNO_3/H_2SO_4, 50 °C, 66 %; c) Me_2NSO_2Cl, Et_3N, toluene, 111 °C, 35 % (a), 33 % (b); d) 1. $LiN(TMS)_2$, THF, −78 °C; 2. CBr_4, THF, −78 °C, 75 % (**a**), 60 % (**b**); e) $BnNH_2$, 0 °C, 92 %; f) Zn, AcOH, H_2O, 25 °C, 94 %; g) dimethyl sulfone, chloroformamidinium chloride, 150 °C, 20 %.

available benzimidazole-5-carboxylic acid (**13**) afforded methyl ester **14**, which was subjected to nitration, resulting in compound **15**. Subsequent protection of the imidazole moiety with the *N*,*N*-dimethylaminosulfonyl group furnished the two regioisomers **16a** (protected at N1) and **16b** (protected at N3) which were separated by column chromatography and identified by X-ray crystal-structure analysis of the latter (Supporting Information). Bromination of regioisomer **16a** at position 2 led to intermediate **17a**, which underwent nucleophilic aromatic substitution with benzylamine to yield **18**. Reduction of the nitro group gave amine **19**, and following cyclization with chlorformamidinium chloride in dimethyl sulfone yielded the desired *lin*-benzoguanine derivative **5**. As a result of the hydrochloric acid liberated during this reaction, deprotection of the imidazole moiety was achieved concurrently with the cyclization reaction.

Fully competitive inhibitory behavior of all the ligands in the base exchange reaction (G34→preQ$_1$) was confirmed by trapping experiments (see the Supporting Information) as previously described[5] and the inhibition constants K_i derived from kinetic measurements.[4] In the trapping experiments, TGT is incubated with an excess of tRNA and the inhibitors are added to validate whether they block tRNA binding in a fully competitive way. In a subsequent sodium dodecyl sulfate (SDS)-polyacrylamide gel electrophoresis (PAGE) analysis, bands for the TGT–tRNA complex are not observed if the inhibitor shows fully competitive behavior. Gratifyingly, all ligands showed fully competitive behavior with binding affinities in the nanomolar range, with the best ones (**10**, **11**) featuring single-digit nanomolar inhibitory constants (Table 1), which are unprecedented activities for inhibitors of TGT enzymes. In addition, the introduction of the morpholino substituent led to the desired free solubility of the best ligand **11** in aqueous buffers.

The X-ray crystal structures of **2**, **3**, **6**, **8**, **10**, and **11** as binary complexes with *Z. mobilis* TGT were solved. Herein we only discuss in detail the structure of the bound naphthyl derivative **8**, solved with a resolution of 1.95 Å (Figure 2).[8]

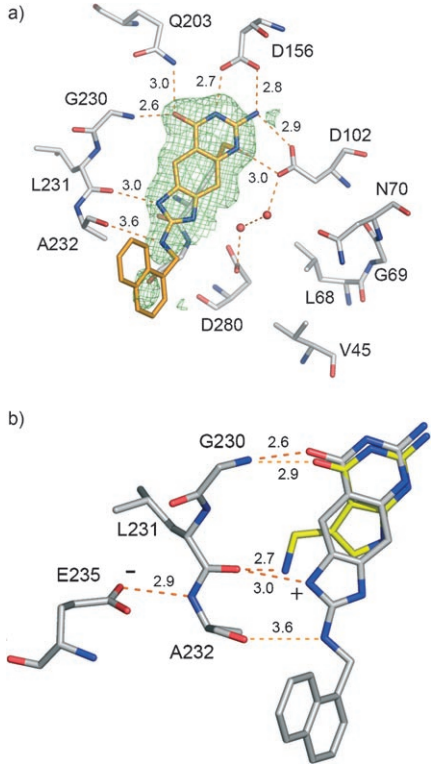

Figure 2. a) Crystal structure of naphthyl-substituted ligand **8** bound to TGT, resolution 1.95 Å. The difference electron density of the compound is shown together with the hydrogen-bonding contacts between the protein and the ligand. Ligand skeleton orange; C gray; O red; N blue; S yellow. b) Superimposition of ligand **8** (gray) and $preQ_1$ (yellow) bound to the active site of TGT. Distances between heavy atoms in Å.

The *lin*-benzoguanine scaffold is well-defined, but the naphthyl substituent is not detected in the difference electron density. It is likely that this part of the ligand is scattered over multiple conformations that point towards the ribose 33 binding pocket. Similarly, the substituents in **6**, **10**, and **11** bound to TGT are not detected in the difference electron density maps. This situation indicates that strong directional interactions have not been established in the environment of the ribose 33 binding pocket, which would lock the substituents in an energetically favorable conformation. Nevertheless, binding free enthalpy should be gained by desolvation of the 2-substituents and the uracil 33 binding pocket. Gains in enthalpy resulting from interactions with the pocket might not be large; on the other hand a substantially unfavorable entropic compensation should also not occur given the apparent residual mobility of these substituents in bound state.

Clearly, the significant increase in affinity of 2-substituted, compared to 4-substituted *lin*-benzoguanines (all of which had activities in the micromolar inhibitory range[4]), can be related to the move of the substituent from the 4- to the 2-position of the heterocyclic platform. This change avoids disturbance of the crucial water network between Asp102 and Asp280. The resolution of the X-ray crystal structure allows location of two crystal water molecules solvating the catalytic residues (Figure 2).

Measured values for the logarithmic distribution coefficient $\log D_{(\text{octanol/water})}$[9] at pH 7.4 (Table 2) clearly show that the increased binding affinity is not at all due to greater lipophilicity resulting from the introduction of the substituents at position 2 of the central scaffold.

Table 2: Binding affinities (inhibition constants K_i [nM]), pK_a values, and log *D* values of selected inhibitors of TGT.

Compd.	K_i [nM]	pK_a	log*D*
1	4100 ± 1000[4]	5.2	−0.05
2	1600 ± 400	5.4	0.11
3	77 ± 12	6.3	−0.33
4	58 ± 36	6.2	−0.07
6	35 ± 9	5.8	1.49
8	55 ± 11	5.9	3.29
11	6 ± 6	6.7	−0.31

A slight increase (factor 2.5) in binding affinity is seen upon expanding the parent *lin*-benzoguanine **1**, ($K_{ic} = 4.1$ μM) by a methyl group in 2-position to give **2** ($K_i = 1.6$ μM). This methyl group forms additional hydrophobic contacts with a small niche next to the side-chain methyl group of Ala232 and the backbone of Gly261.

A larger increase in binding affinity, down to the single-digit nanomolar range, is observed for the compounds bearing amino substituents in position 2. The crystal structures show an additional hydrogen bond between the exocyclic amino group and the carbonyl group of Ala232 ($d(\text{N}\cdots\text{O}) = 2.8$ Å in the complex with **3** (not shown) and 3.6 Å with **8** (Figure 2)). More importantly however, this exocyclic amino group increases the basicity of the imidazole ring. The now guanidine-like 2-aminoimidazol group is protonated, thereby bearing positive charge and enabling strong charge-assisted hydrogen bonding.

In the structure of the complex of TGT and $preQ_1$, which was obtained by co-crystallization, the carbonyl group of the peptide bond between Leu231 and Ala232 is oriented towards the exocyclic basic aminomethyl group of the modified nucleobase (Figure 2b).[10] At the same time, the N–H group of this peptide bond interacts with the side chain of Glu235 and stabilizes this orientation. At physiological pH value, the aminomethyl group should be protonated whereas the side chain of Glu235 should be deprotonated. This way, a strong charge-assisted hydrogen-bonding network with two ionic hydrogen bonds ($d(\text{O}^-_{\text{E235}}\cdots\text{HN}_{\text{Ala232}}) = 2.7$ Å (distance between heavy atoms) and $d(\text{C}{=}\text{O}_{\text{Leu231}}\cdots\text{HN}^+_{\text{preqQ1}}) = 2.9$ Å) is formed (Figure 2).[11] In general, charge-assistance is thought to contribute significantly to binding affinity.[12] We therefore hypothesized that the 2-aminoimidazole ring in the most potent of our ligands could also be protonated, thereby establishing a similar charge-assisted hydrogen-bonding network. In other words, an ionic

rather than a neutral hydrogen bond would form between N1 of the aminoimidazolium ring and C=O_{Leu231}.

To verify this assumption, the pK_a values of some representative ligands were determined by photometric titration.[9,13] Table 2 shows the relevant pK_a values assigned to the protonation of the imidazole rings in the ligands; the entire set of pK_a data for each molecule can be found in the the Supporting Information. The pK_a value is indeed substantially increased upon introduction of an amino substituent in position 2: it changes from *lin*-benzoguanine (**1**, pK_a = 5.2) and its methyl derivative **2** (5.4) to substantially higher values between 5.9 (**6**) and 6.7 (**11**). Hence, under the conditions of the binding assay at pH 7.3, the 2-amino-substituted imidazole moiety of the ligands is more readily protonated. Furthermore, in the polar environment of the binding pocket an additional pK_a shift is expected stabilizing the charged state. To support such considerations we performed Poisson–Boltzmann calculations using our recently introduced PEOE-PB charge model for protein–ligand complexes.[14–16] These calculations provide good evidence that the actual pK_a values of the bound amino-substituted ligands are shifted by 1–2 pK_a units (logarithmic scale) to higher values, so that the ligands should be fully protonated once accommodated in the active site (for details on pK_a calculations see the Supporting Information). We therefore propose that the hydrogen bond between N1 of **8** and C=O_{Leu231} (d = 3.0 Å) has ionic character (Figure 2).

In summary, we have reported the synthesis and biological evaluation of the most potent small-molecule inhibitors of TGT known to date. Strong evidence is provided that the 2-aminoimidazole moieties in the most effective ligands are protonated and that complexation is enhanced by charge-assisted hydrogen bonding between protein and ligand as found for the complexation with the natural substrate $preQ_1$. The synthesis of these inhibitors with single-figure nanomolar inhibition constants is an important step towards the development of new, specific drugs against Shigellosis.

Received: July 3, 2007
Published online: September 27, 2007

Keywords: drug design · glycosylases · hydrogen bonds · inhibitors · shigellosis · TGT

[1] C. Romier, J. E. W. Meyer, D. Suck, *FEBS Lett.* **1997**, *416*, 93–98.
[2] D. Iwata-Reuyl, *Bioorg. Chem.* **2003**, *31*, 24–43.
[3] N. Okada, C. Sasakawa, T. Tobe, M. Yamada, S. Nagai, K. A. Talukder, K. Komatsu, S. Kanegasaki, M. Yoshikawa, *Mol. Microbiol.* **1991**, *5*, 187–195.
[4] E. A. Meyer, N. Donati, M. Guillot, W. B. Schweizer, F. Diederich, B. Stengl, R. Brenk, K. Reuter, G. Klebe, *Helv. Chim. Acta* **2006**, *89*, 573–597.
[5] B. Stengl, E. A. Meyer, A. Heine, R. Brenk, F. Diederich, G. Klebe, *J. Mol. Biol.* **2007**, *370*, 492–511.
[6] W. Xie, X. Liu, R. H. Huang, *Nat. Struct. Biol.* **2003**, *10*, 781–788.
[7] P. R. Gerber, K. Müller, *J. Comput.-Aided Mol. Des.* **1995**, *9*, 251–268.
[8] B. Stengl, Doctoral Dissertation, Philipps-Universität, Marburg, **2006**.
[9] J. Olsen, P. Seiler, B. Wagner, H. Fischer, T. Tschopp, U. Obst-Sander, D. W. Banner, M. Kansy, K. Müller, F. Diederich, *Org. Biomol. Chem.* **2004**, *2*, 1339–1352.
[10] R. Brenk, M. T. Stubbs, A. Heine, K. Reuter, G. Klebe, *ChemBioChem* **2003**, *4*, 100–111.
[11] B. Stengl, K. Reuter, G. Klebe, *ChemBioChem* **2005**, *6*, 1066–1077.
[12] S. H. Reich, M. A. Fuhry, D. Nguyen, M. J. Pino, K. M. Welsh, S. Webber, C. A. Janson, S. R. Jordan, D. A. Matthews, W. W. Smith, *J. Med. Chem.* **1992**, *35*, 847–858.
[13] For a recent review on tuning and predicting amine basicities, see: M. Morgenthaler, E. Schweizer, A. Hoffmann-Röder, F. Benini, R. E. Martin, G. Jaeschke, B. Wagner, H. Fischer, S. Bendels, D. Zimmerli, J. Schneider, F. Diederich, M. Kansy, K. Müller, *ChemMedChem* **2007**, *2*, 1100–1115.
[14] P. Czodrowski, I. Dramburg, C. A. Sotriffer, G. Klebe, *Proteins Struct. Funct. Bioinf.* **2006**, *65*, 424–437.
[15] P. Czodrowski, C. A. Sotriffer, G. Klebe, *J. Mol. Biol.* **2007**, *367*, 1347–1356.
[16] P. Czodrowski, C. A. Sotriffer, G. Klebe, *J. Chem. Inf. Model.* **2007**, *47*, 1590–1598.
[17] W. DeLano, **2006**, www.pymol.org.

